

Fast Adaptation Nonlinear Observer for SLAM

Trevor P. Drayton, Abdul A. Jaiyeola, Nazmul Hoque, Mikhayla Maurer, and Hashim A. Hashim
Software Engineering

Department of Engineering and Applied Science

Thompson Rivers University, Kamloops, British Columbia, Canada, V2C-0C8

draytont10@mytru.ca, jaiyeolaa17@mytru.ca, hoquen18@mytru.ca, maurerm18@mytru.ca and hhashim@tru.ca

Abstract—The process of simultaneously mapping the environment in three dimensional (3D) space and localizing a moving vehicle’s pose (orientation and position) is termed Simultaneous Localization and Mapping (SLAM). SLAM is a core task in robotics applications. In the SLAM problem, each of the vehicle’s pose and the environment are assumed to be completely unknown. This paper takes the conventional SLAM design as a basis and proposes a novel approach that ensures fast adaptation of the nonlinear observer for SLAM. Due to the fact that the true SLAM problem is nonlinear and is modeled on the Lie group of $\text{SLAM}_n(3)$, the proposed observer for SLAM is nonlinear and modeled on $\text{SLAM}_n(3)$. The proposed observer compensates for unknown bias attached to velocity measurements. The results of the simulation illustrate the robustness of the proposed approach.

I. INTRODUCTION

SIMULTANEOUS Localization and Mapping (SLAM) is a well-established problem in robotics and has been an active area of research over the past three decades [1]–[7]. The SLAM problem concerns a vehicle whose 1) pose (orientation and position) is unknown, traveling within 2) an unknown environment. This task is particularly important in GPS-denied applications, for instance, indoor applications, surveillance, and others. The localization and mapping process are performed via a set of measurements, typically, angular and translational velocities of the vehicle, and landmark measurements. It is apparent that sensor measurements are characterized by irregular behavior and the presence of uncertainties. Therefore, robust observers for SLAM are indispensable.

SLAM observation is traditionally tackled using Gaussian filters or nonlinear observers. Gaussian filters allow to observe the vehicle’s pose along with the surrounding landmarks. Examples of Gaussian filters for SLAM include the MonoSLAM approach that utilizes a single camera and real-time data [5], FastSLAM based on a scalable approach [8], extended Kalman filter (EKF) [9], and particle filter [4], among others. The Gaussian filters take a probabilistic approach to uncertainties present in measurements. It is worth mentioning that SLAM is an open problem and common issues are consistency [10], solution complexity [11], and landmarks in motion. However, the SLAM problem is highly nonlinear and constitutes a dual observation process comprised of pose and environment observation. Pose of a vehicle is composed of: orientation (attitude) and position. While attitude is represented relative

to the Special Orthogonal Group $\text{SO}(3)$ [12], [13], pose is described relative to the Special Euclidean Group $\text{SE}(3)$ [14]–[16]. Gaussian filters fail to account for the high nonlinearity of the SLAM problem. As such, SLAM observation problem is best addressed using nonlinear observers.

Recent advances in the area of nonlinear observers evolved directly on $\text{SO}(3)$ [12], [13], [17], [18] and $\text{SE}(3)$ [14], [15], [19], [20], which opened the door to proposing nonlinear observers for SLAM. An early study that proposed using the Lie group of $\text{SE}(3)$ as the true representation of the SLAM problem was presented in [21]. It was followed by two-staged observers, with nonlinear observer for pose estimation and Kalman filter for landmark estimation [22]. The true SLAM problem is nonlinear and is modeled on the Lie group of $\text{SLAM}_n(3)$. Nonlinear observers for SLAM on $\text{SLAM}_n(3)$ have been proposed in [1], [6], [7]. The innovative component of the observers in [6], [7] consists in the use of constant gains which do not allow for fast adaptation. Accordingly, this paper proposes a nonlinear observer for SLAM on $\text{SLAM}_n(3)$ that follows the structure of the work in [1], [6] with the main contributions as listed below:

- 1) A nonlinear observer for SLAM with fast adaptation that uses the available measurements of angular velocity, translational velocity, and landmarks.
- 2) Exponential convergence of the error component is guaranteed.
- 3) The closed loop error signals are guaranteed to be uniformly ultimately bounded.

The remainder of the paper is organized as follows: Section II introduces the nomenclature, overview of $\text{SO}(3)$ and $\text{SE}(3)$, and math notation. Section III defines the SLAM problem, available sensor measurements, and the true motion kinematics. Section IV presents nonlinear observer for SLAM on $\text{SLAM}_n(3)$ with fast adaptation. Section V reveals the robustness of the proposed observer. Lastly, the conclusion is contained in Section VI.

This work was supported in part by Thompson Rivers University Internal research fund, RGS-2020/21 IRF, # 102315.

II. PRELIMINARIES AND MATH NOTATION

A. Nomenclature

$\{\mathcal{I}\}$	Inertial-frame
$\{\mathcal{B}\}$	Body-frame
\mathbb{R}	Set of real numbers
\mathbb{R}_+	Set of nonnegative real numbers
$\mathbb{R}^{n \times m}$	Set of real numbers with dimension n -by- m
$\ y\ $	Euclidean norm $\ y\ = \sqrt{y^\top y}$, $\forall y \in \mathbb{R}^n$
$\mathbb{SO}(3)$	Special Orthogonal Group of order 3
$\mathbb{SE}(3)$	Special Euclidean Group of order 3

B. Preliminaries

The Special Orthogonal Group $\mathbb{SO}(3)$ is described by

$$\mathbb{SO}(3) = \{R \in \mathbb{R}^{3 \times 3} \mid RR^\top = \mathbf{I}_3, \det(R) = +1\}$$

Note that $R \in \mathbb{SO}(3)$ is expressed relative to $\{\mathcal{B}\}$. The Special Euclidean Group $\mathbb{SE}(3)$ is defined as

$$\mathbb{SE}(3) = \left\{ \mathbf{T} = \begin{bmatrix} R & P \\ 0_{1 \times 3} & 1 \end{bmatrix} \in \mathbb{R}^{4 \times 4} \mid R \in \mathbb{SO}(3), P \in \mathbb{R}^3 \right\}$$

where $P \in \mathbb{R}^3$ refers to rigid-body's position. P is defined relative to $\{\mathcal{I}\}$. $\mathbf{T} \in \mathbb{SE}(3)$ is commonly known as a homogeneous transformation matrix that describes rigid-body's pose and is given by

$$\mathbf{T} = \begin{bmatrix} R & P \\ 0_{1 \times 3} & 1 \end{bmatrix} \in \mathbb{SE}(3) \quad (1)$$

$\mathfrak{so}(3)$ is the Lie-algebra of $\mathbb{SO}(3)$ with

$$\mathfrak{so}(3) = \left\{ [y]_\times \in \mathbb{R}^{3 \times 3} \mid [y]_\times^\top = -[y]_\times, y \in \mathbb{R}^3 \right\} \quad (2)$$

where $[y]_\times$ refers to a skew symmetric matrix such that

$$[y]_\times = \begin{bmatrix} 0 & -y_3 & y_2 \\ y_3 & 0 & -y_1 \\ -y_2 & y_1 & 0 \end{bmatrix} \in \mathfrak{so}(3), \quad y = \begin{bmatrix} y_1 \\ y_2 \\ y_3 \end{bmatrix}$$

$\mathfrak{se}(3)$ is the Lie-algebra of $\mathbb{SE}(3)$ where

$$\mathfrak{se}(3) = \left\{ [U]_\wedge \in \mathbb{R}^{4 \times 4} \mid \exists u_1, u_2 \in \mathbb{R}^3 : [U]_\wedge = \begin{bmatrix} [u_1]_\times & u_2 \\ \mathbf{0}_3 & 0 \end{bmatrix} \right\}$$

$[\cdot]_\wedge$ is a wedge operator that follows $[\cdot]_\wedge : \mathbb{R}^6 \rightarrow \mathfrak{se}(3)$ such that

$$[U]_\wedge = \begin{bmatrix} [u_1]_\times & u_2 \\ \mathbf{0}_3 & 0 \end{bmatrix} \in \mathfrak{se}(3), \quad U = \begin{bmatrix} u_1 \\ u_2 \end{bmatrix} \in \mathbb{R}^6 \quad (3)$$

Let $\|R\|_1$ be a normalized Euclidean distance of $R \in \mathbb{SO}(3)$ where

$$\|R\|_1 = \frac{1}{4} \text{Tr} \{ \mathbf{I}_3 - R \} \in [0, 1] \quad (4)$$

For more information of attitude representation on $\mathbb{SO}(3)$ visit [12], [13] and pose representation on $\mathbb{SE}(3)$ visit [14], [15].

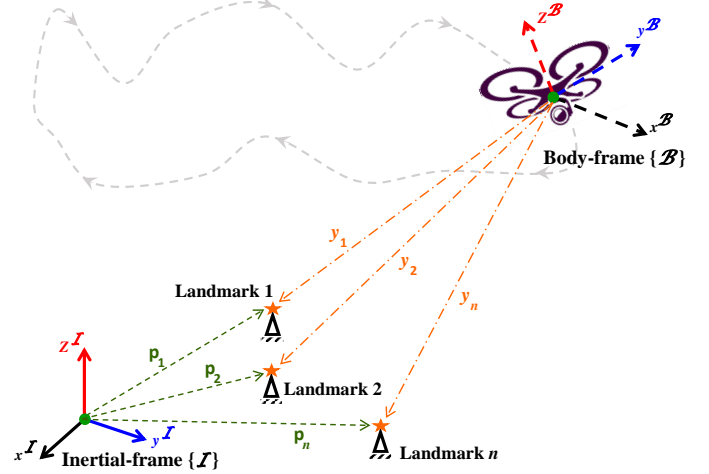


Fig. 1. SLAM observation problem [1], [7].

III. PROBLEM FORMULATION

SLAM estimation problem concerns simultaneous observation of the vehicle's pose and landmarks within the environment. Fig. 1 illustrates the SLAM observation problem.

Define $R \in \mathbb{SO}(3)$ as the rigid-body's attitude and $P \in \mathbb{R}^3$ as the rigid-body's translation for all $R \in \{\mathcal{B}\}$ and $P \in \{\mathcal{I}\}$. Assume that the map contains a family of n landmarks, and let p_i represent the i th landmark location where $p_i \in \{\mathcal{I}\}$ for all $i = 1, 2, \dots, n$. The observation problem can be solved given a set of measurements in the body-frame. The measurement of p_i is given by

$$y_i = R^\top (p_i - P) + b_i^y + n_i^y \in \mathbb{R}^3 \quad (5)$$

where R , refers to the rigid-body's orientation, P describes its translation, and p_i refers to the landmark's location. Additionally, b_i^y defines unknown constant bias and n_i^y defines unknown random noise attached to the measurement with $y_i, b_i^y, n_i^y \in \{\mathcal{B}\}$.

Assumption 1. Assume three or more landmarks are available for measurement.

The true motion kinematics of the rigid-body's attitude and position and a group of n -landmarks are given by [1], [7]

$$\begin{aligned} \dot{\mathbf{T}} &= \mathbf{T} [U]_\wedge \\ \dot{p}_i &= R v_i, \quad \forall i = 1, 2, \dots, n \end{aligned}$$

and in detailed form

$$\begin{cases} \dot{R} &= R [\Omega]_\times \\ \dot{P} &= R V \\ \dot{p}_i &= R v_i, \quad \forall i = 1, 2, \dots, n \end{cases} \quad (6)$$

where $U = [\Omega^\top, V^\top]^\top$, $\Omega \in \mathbb{R}^3$ defines the rigid-body's true angular velocity, $V \in \mathbb{R}^3$ defines its true translational velocity, and $v_i \in \mathbb{R}^3$ defines the true linear velocity of the i th

landmark. Note that each of $\Omega, V, v_i \in \{\mathcal{B}\}$. The measurements of angular and translational velocity can be described as

$$\begin{cases} \Omega_m &= \Omega + b_\Omega + n_\Omega \in \mathbb{R}^3 \\ V_m &= V + b_V + n_V \in \mathbb{R}^3 \end{cases} \quad (7)$$

where b_Ω defines unknown constant bias and n_Ω denotes unknown random noise attached to the angular velocity, while b_V defines unknown constant bias and n_V denotes unknown random noise attached to the translational velocity. Note that the measurements of angular and translational velocities are expressed with respect to $\{\mathcal{B}\}$. All landmarks are assumed to be fixed, thus $v_i = 0_{3 \times 1} \forall i = 1, 2, \dots, n$.

Assumption 2. (Uniform boundedness of b_Ω and b_V) Assume that b_Ω and b_V are subset of Λ_b with $b_\Omega, b_V \in \Lambda_b \subset \mathbb{R}^3$, where b_Ω and b_V are ultimately bounded by Γ .

A. Error in Attitude, Position, and Landmark

Consider \hat{R} to be an estimate of the true orientation (R), \hat{P} an estimate of the true rigid-body's position (P), and \hat{p}_i an estimate of the true location of the i th landmark (p_i). Consider defining the error in pose observation as

$$\begin{aligned} \tilde{T} &= \hat{T}T^{-1} = \begin{bmatrix} \hat{R} & \hat{P} \\ \mathbf{0}_3^\top & 1 \end{bmatrix} \begin{bmatrix} R^\top & -R^\top P \\ \mathbf{0}_3^\top & 1 \end{bmatrix} \\ &= \begin{bmatrix} \tilde{R} & \tilde{P} \\ \mathbf{0}_3^\top & 1 \end{bmatrix} \end{aligned} \quad (8)$$

which is equivalent to

$$\begin{cases} \tilde{R} &= \hat{R}R^\top \\ \tilde{P} &= \hat{P} - \tilde{R}P \end{cases} \quad (9)$$

Consider defining the error in the i th landmark observation as

$$\begin{aligned} \begin{bmatrix} e_i \\ 0 \end{bmatrix} &= \begin{bmatrix} \hat{p}_i \\ 1 \end{bmatrix} - \begin{bmatrix} \hat{R} & \hat{P} \\ \mathbf{0}_3^\top & 1 \end{bmatrix} \begin{bmatrix} y_i \\ 1 \end{bmatrix}, \quad \forall i = 1, 2, \dots, n \\ &= \begin{bmatrix} \hat{p}_i \\ 1 \end{bmatrix} - \begin{bmatrix} \hat{R} & \hat{P} \\ \mathbf{0}_3^\top & 1 \end{bmatrix} \begin{bmatrix} R^\top (p_i - P) \\ 1 \end{bmatrix} \\ &= \begin{bmatrix} \hat{p}_i \\ 1 \end{bmatrix} - \tilde{T} \begin{bmatrix} p_i \\ 1 \end{bmatrix} \\ &= \begin{bmatrix} \tilde{p}_i - \tilde{P} \\ 0 \end{bmatrix} \end{aligned} \quad (10)$$

where $\tilde{p}_i = \hat{p}_i - \tilde{R}p_i$ and $\tilde{P} = \hat{P} - \tilde{R}P$. Define \hat{b}_Ω as an estimate of the unknown constant bias attached to the angular velocity and \hat{b}_V as an estimate of the unknown constant bias attached to the translational velocity. Also, consider defining the bias error as follows:

$$\begin{cases} \tilde{b}_\Omega &= b_\Omega - \hat{b}_\Omega \\ \tilde{b}_V &= b_V - \hat{b}_V \end{cases} \quad (11)$$

Definition 1. Define $x \in \mathbb{R}^3$ as a unit-axis rotating at an angle of $\theta \in \mathbb{R}$ in a 2-sphere \mathbb{S}^2 . Angle-axis representation is one of the methods of attitude representation which has the map of $\mathcal{R}_\theta : \mathbb{R} \times \mathbb{R}^3 \rightarrow \mathbb{SO}(3)$ [23], [24]

$$\mathcal{R}_\theta(\theta, x) = \mathbf{I}_3 + \sin(\theta) [x]_\times + (1 - \cos(\theta)) [x]_\times^2 \in \mathbb{SO}(3)$$

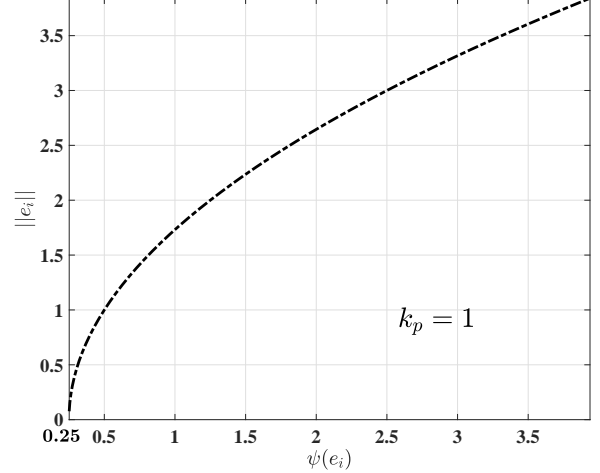


Fig. 2. Illustrative performance of $\psi(e_i)$: $k_p/4 \leq \psi(e_i) < \infty$

From (10), and consistently with Lemma 4 [24], consider defining

$$\begin{aligned} \theta_i &= 2 \tan^{-1}(\|e_i\|) \\ x_i &= \cot\left(\frac{\theta_i}{2}\right) e_i \end{aligned}$$

The following mapping is obtained [24]

$$\mathcal{R}_{e(i)} = \mathbf{I}_3 + \sin(\theta_i) [x_i]_\times + (1 - \cos(\theta_i)) [x_i]_\times^2 \quad (12)$$

Remark 1. Recall the definition of the normalized Euclidean distance in (4). From (12) and Definition 1, one finds $-1 \leq \text{Tr}\{\mathcal{R}_{e(i)}\} \leq 3$ such that $\text{Tr}\{\mathcal{R}_{e(i)}\} \rightarrow -1$ as $e_i \rightarrow \infty$ and $\text{Tr}\{\mathcal{R}_{e(i)}\} \rightarrow 3$ as $e_i \rightarrow 0$.

Definition 2. (Fast adaptation) Based on Definition 1 and Remark 1, define the following positive function $\psi : \mathbb{SO}(3) \rightarrow \mathbb{R}_+$

$$\psi(e_i) = \frac{k_p}{1 + \text{Tr}\{\mathcal{R}_{e(i)}\}} \quad (13)$$

The value of the function $\psi(e_i)$ in (13) becomes increasingly aggressive with $\psi(e_i) \rightarrow +\infty$ as $e_i \rightarrow \pm\infty$ and $\psi(e_i) \rightarrow k_p/4$ as $e_i \rightarrow 0$, visit [24]. The behavior of the proposed function in (13) is illustrated in Fig. 2.

IV. NONLINEAR OBSERVER DESIGN

Consider the following nonlinear observer design:

$$\begin{cases} \dot{\hat{R}} &= \hat{R} \left[\Omega_m - \hat{b}_\Omega - W_\Omega \right]_\times \\ \dot{\hat{P}} &= \hat{R} \left(V_m - \hat{b}_V - W_V \right) \\ \theta_i &= 2 \tan^{-1}(\|e_i\|), \quad x_i = \cot\left(\frac{\theta_i}{2}\right)e_i \\ \mathcal{R}_{e(i)} &= \mathbf{I}_3 + \sin(\theta_i) [x_i]_\times + (1 - \cos(\theta_i)) [x_i]_\times^2 \\ \psi(e_i) &= \frac{k_p}{1 + \text{Tr}\{\mathcal{R}_{e(i)}\}} \\ \dot{\hat{p}}_i &= -\psi(e_i)e_i, \quad \forall i = 1, 2, \dots, n \\ \dot{\hat{b}}_\Omega &= -\sum_{i=1}^n \frac{\Gamma}{\alpha_i} [y_i]_\times \hat{R}^\top e_i \\ \dot{\hat{b}}_V &= -\sum_{i=1}^n \frac{\Gamma}{\alpha_i} \hat{R}^\top e_i \\ W_\Omega &= -\sum_{i=1}^n \frac{k_w}{\alpha_i} [y_i]_\times \hat{R}^\top e_i \\ W_V &= -\sum_{i=1}^n \frac{k_w}{\alpha_i} \hat{R}^\top e_i \end{cases} \quad (14)$$

where $k_w \in \mathbb{R}$, $k_p \in \mathbb{R}$, $\Gamma \in \mathbb{R}^{3 \times 3}$, and $\alpha_i \in \mathbb{R}$ are positive constants, W_Ω and W_V are correction factors, and \hat{b}_Ω and \hat{b}_V are the estimates of b_Ω and b_V , respectively.

Theorem 1. Consider the true motion kinematics in (6), landmark measurements ($y_i = R^\top (p_i - P)$) for all $i = 1, 2, \dots, n$, and angular velocity measurement $\Omega_m = \Omega + b_\Omega$, and translational velocity measurement $V_m = V + b_V$ as in (7). Assume that Assumption 1 is met. Consider the observer design to be as in (14). Define the set

$$\mathcal{S} = \left\{ (e_1, e_2, \dots, e_n) \in \mathbb{R}^3 \times \mathbb{R}^3 \times \dots \times \mathbb{R}^3 \mid e_i = \mathbf{0}_3 \forall i = 1, 2, \dots, n \right\} \quad (15)$$

Then

- 1) e_i in (10) exponentially approaches \mathcal{S} , and
- 2) the error in attitude and position $\hat{R} \rightarrow R_c$ and $\hat{P} \rightarrow P_c$ as $t \rightarrow \infty$ where $R_c \in \mathbb{SO}(3)$ refers to a constant matrix and $P_c \in \mathbb{R}^3$ refers to a constant vector.

Proof. From (8), one has

$$\begin{aligned} \dot{\hat{T}} &= \dot{\hat{T}}\hat{T}^{-1} + \hat{T}\dot{\hat{T}}^{-1} \\ &= \hat{T} \left[\tilde{b}_U - W_U \right]_\wedge \hat{T}^{-1} \hat{T} \end{aligned} \quad (16)$$

where $\dot{\hat{T}}^{-1} = -\hat{T}^{-1}\dot{\hat{T}}\hat{T}^{-1}$. Thereby, the error dynamics of (10) are equivalent to

$$\begin{aligned} \begin{bmatrix} \dot{e}_i \\ 0 \end{bmatrix} &= \begin{bmatrix} \dot{\hat{p}}_i \\ 0 \end{bmatrix} - \dot{\hat{T}} \begin{bmatrix} p_i \\ 1 \end{bmatrix} - \hat{T} \dot{\hat{p}}_i \\ &= \begin{bmatrix} \dot{\hat{p}}_i \\ 0 \end{bmatrix} - \hat{T} \left[\tilde{b}_U - W_U \right]_\wedge \hat{T}^{-1} \hat{T} \begin{bmatrix} p_i \\ 1 \end{bmatrix} \end{aligned} \quad (17)$$

From (16), one finds

$$\hat{T} \left[\tilde{b}_U \right]_\wedge \hat{T}^{-1} = \begin{bmatrix} \hat{R} \tilde{b}_\Omega \\ \hat{R} \tilde{b}_V + \left[\hat{P} \right]_\times \hat{R} \tilde{b}_\Omega \end{bmatrix}_\wedge \in \mathfrak{se}(3) \quad (18)$$

where for $x \in \mathbb{R}^3$ and $R \in \mathbb{SO}(3)$, $[Rx]_\times = R[x]_\times R^\top$. Accordingly, the result in (18) is equivalent to

$$\hat{T} \left[\tilde{b}_U \right]_\wedge \hat{T}^{-1} = \left[\begin{bmatrix} \hat{R} & \mathbf{0}_{3 \times 3} \\ \left[\hat{P} \right]_\times & \hat{R} \end{bmatrix} \begin{bmatrix} \tilde{b}_\Omega \\ \tilde{b}_V \end{bmatrix} \right]_\wedge \quad (19)$$

which shows that

$$\hat{T} \left[\tilde{b}_U \right]_\wedge \hat{T}^{-1} \hat{T} \tilde{p}_i = \begin{bmatrix} -\hat{R} [y_i]_\times & \hat{R} \\ \mathbf{0}_3^\top & \mathbf{0}_3^\top \end{bmatrix} \begin{bmatrix} \tilde{b}_\Omega \\ \tilde{b}_V \end{bmatrix} \quad (20)$$

Therefore, it can be concluded that the error dynamics are

$$\dot{e}_i = \dot{\hat{p}}_i - \begin{bmatrix} -\hat{R} [y_i]_\times & \hat{R} \\ \tilde{b}_\Omega - W_\Omega \\ \tilde{b}_V - W_V \end{bmatrix} \quad (21)$$

Consider the candidate Lyapunov function $\mathbf{V} = \mathbf{V}(e_1, \dots, e_n, \tilde{b}_\Omega, \tilde{b}_V)$ defined as follows:

$$\mathbf{V} = \sum_{i=1}^n \frac{1}{2\alpha_i} e_i^\top e_i + \frac{1}{2} \tilde{b}_\Omega^\top \Gamma^{-1} \tilde{b}_\Omega + \frac{1}{2} \tilde{b}_V^\top \Gamma^{-1} \tilde{b}_V \quad (22)$$

The time derivative of (22) becomes

$$\begin{aligned} \dot{\mathbf{V}} &= \sum_{i=1}^n \frac{1}{\alpha_i} e_i^\top \dot{e}_i - \tilde{b}_\Omega^\top \Gamma^{-1} \dot{\tilde{b}}_\Omega - \tilde{b}_V^\top \Gamma^{-1} \dot{\tilde{b}}_V \\ &= -\sum_{i=1}^n \frac{1}{\alpha_i} e_i^\top \begin{bmatrix} -\hat{R} [y_i]_\times & \hat{R} \\ \tilde{b}_\Omega - W_\Omega \\ \tilde{b}_V - W_V \end{bmatrix} \\ &\quad + \sum_{i=1}^n \frac{1}{\alpha_i} e_i^\top \dot{\hat{p}}_i - \tilde{b}_\Omega^\top \Gamma^{-1} \dot{\tilde{b}}_\Omega - \tilde{b}_V^\top \Gamma^{-1} \dot{\tilde{b}}_V \\ &= \sum_{i=1}^n \frac{1}{\alpha_i} e_i^\top \hat{R} [y_i]_\times (\tilde{b}_\Omega - W_\Omega) \\ &\quad - \sum_{i=1}^n \frac{1}{\alpha_i} e_i^\top \hat{R} (\tilde{b}_V - W_V) \\ &\quad + \sum_{i=1}^n \frac{1}{\alpha_i} e_i^\top \dot{\hat{p}}_i - \tilde{b}_\Omega^\top \Gamma^{-1} \dot{\tilde{b}}_\Omega - \tilde{b}_V^\top \Gamma^{-1} \dot{\tilde{b}}_V \end{aligned} \quad (23)$$

Replacing W_Ω , W_V , $\dot{\tilde{b}}_\Omega$, $\dot{\tilde{b}}_V$, and $\dot{\hat{p}}_i$ with their definitions in (14) leads to

$$\dot{\mathbf{V}} \leq -\sum_{i=1}^n \frac{\psi(e_i)}{\alpha_i} \|e_i\|^2 - k_w \left\| \sum_{i=1}^n \frac{e_i}{\alpha_i} \right\|^2 \quad (24)$$

From (24), $\dot{\mathbf{V}}$ is negative for all $e_i \neq 0$ and \mathbf{V} is equal to zero at $e_i = \mathbf{0}_{3 \times 1}$. Thus, the inequality in (24) shows that e_i is regulated exponentially to the set \mathcal{S} in (15). In view of Barbalat Lemma, $\dot{\mathbf{V}}$ is negative, continuous, and converges to zero indicating that \tilde{b}_Ω and \tilde{b}_V are bounded. As such, $\hat{R} \rightarrow R_c$ and $\hat{P} \rightarrow P_c$ as $t \rightarrow \infty$ completing the proof. \square

The discrete implementation of the observer in (14) is given by

$$\begin{cases} \hat{T}[k+1] &= \hat{T}[k] \exp \left(\begin{bmatrix} \Omega_m[k] - \hat{b}_\Omega[k] - W_\Omega[k] \\ V_m[k] - \hat{b}_V[k] - W_V[k] \end{bmatrix}_\wedge \Delta t \right) \\ \theta_i &= 2 \tan^{-1}(\|e_i[k]\|), \quad x_i = \cot\left(\frac{\theta_i}{2}\right)e_i[k] \\ \mathcal{R}_{e(i)} &= \mathbf{I}_3 + \sin(\theta_i) [x_i]_\times + (1 - \cos(\theta_i)) [x_i]_\times^2 \\ \psi(e_i) &= \frac{k_p}{1 + \text{Tr}\{\mathcal{R}_{e(i)}\}} \\ \hat{p}_i[k+1] &= \hat{p}_i[k] - \Delta t \psi(e_i) e_i[k], \quad \forall i = 1, 2, \dots, n \\ \hat{b}_\Omega[k+1] &= \hat{b}_\Omega[k] - \Delta t \sum_{i=1}^n \frac{\Gamma}{\alpha_i} [y_i[k]]_\times \hat{R}^\top [k] e_i[k] \\ \hat{b}_V[k+1] &= \hat{b}_V[k] - \sum_{i=1}^n \frac{\Gamma}{\alpha_i} \hat{R}^\top [k] e_i[k] \\ W_\Omega &= -\sum_{i=1}^n \frac{k_w}{\alpha_i} [y_i[k]]_\times \hat{R}^\top [k] e_i[k] \\ W_V &= -\sum_{i=1}^n \frac{k_w}{\alpha_i} \hat{R}^\top [k] e_i[k] \end{cases} \quad (25)$$

V. SIMULATION RESULTS

This section reveals the robustness of the proposed nonlinear observer with fast adaptation for SLAM on the Lie group of $\text{SLAM}_n(3)$. Consider the following set of data, initialization parameters, and measurement bias:

$$\left\{ \begin{array}{l} \Omega = [0, 0, 0.3]^\top (\text{rad/sec}) \\ V = [2.5, 0, 0]^\top (\text{m/sec}) \\ R(0) = \mathbf{I}_3 \\ P(0) = [0, 0, 6]^\top \\ p_1 = [7, 7, 0]^\top \\ p_2 = [-7, 7, 0]^\top \\ p_3 = [7, -7, 0]^\top \\ p_4 = [-7, -7, 0]^\top \\ b_\Omega = [0.09, -0.15, -0.1]^\top (\text{rad/sec}) \\ b_V = [0.09, 0.06, -0.07]^\top (\text{m/sec}) \end{array} \right.$$

Consider the initial estimates of attitude, position, and landmark locations to be

$$\begin{aligned} \hat{R}(0) &= \mathbf{I}_3, \quad \hat{P}(0) = 0_{3 \times 1} \\ \hat{p}_1(0) &= \hat{p}_2(0) = \hat{p}_3(0) = \hat{p}_4(0) = 0_{3 \times 1} \end{aligned}$$

Consider selecting the design parameters as follows: $\alpha_i = 0.1$, $\Gamma = 30\mathbf{I}_3$, $k_p = 1$, and $k_w = 2$, while the initial estimates of the biases are $\hat{b}_\Omega(0) = \hat{b}_V(0) = 0_{3 \times 1}$ for all $i = 1, 2, 3, 4$.

Fig. 3 illustrates the output performance of the proposed observer against the true trajectory. The true performance is depicted in black center-line with final destinations depicted as black circles. The estimated performance is shown in red dash-line and blue center-line, while the estimated positions of the final destinations are depicted as red and blue stars \star . Fig. 3 reveals strong estimation capabilities of the proposed observer in localizing the unknown pose of the vehicle as well as mapping the unknown environment.

Fig. 4 reveals asymptotic and fast convergence of e_i to the origin from large error in initialization. Likewise, Fig. 5 demonstrates fast convergence of $\|p_i - \hat{p}_i\|$ from large error in initialization to the close neighborhood of the origin.

VI. CONCLUSION

A nonlinear observer for Simultaneous Localization and Mapping (SLAM) modeled on the Lie group of $\text{SLAM}_n(3)$ is proposed. The observer follows the structure of the true SLAM problem. The proposed observer compensates for the unknown bias attached to angular and translational velocities. The proposed observer can be easily implemented on a vehicle given the availability of velocity and landmark measurements. Numerical results revealed the observer's ability to concurrently map the unknown environment and obtain the vehicle's pose.

ACKNOWLEDGMENT

The authors would like to thank **Maria Shaposhnikova** for proofreading the article.

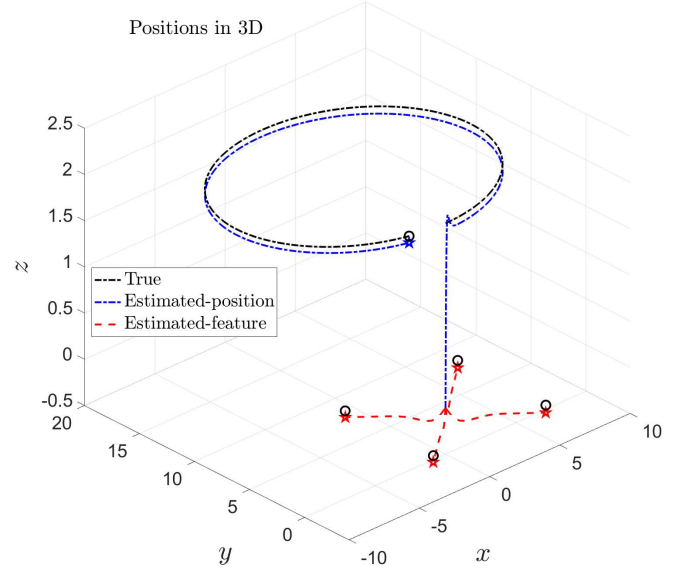


Fig. 3. Output performance of fast adaptation nonlinear observer for SLAM vs True

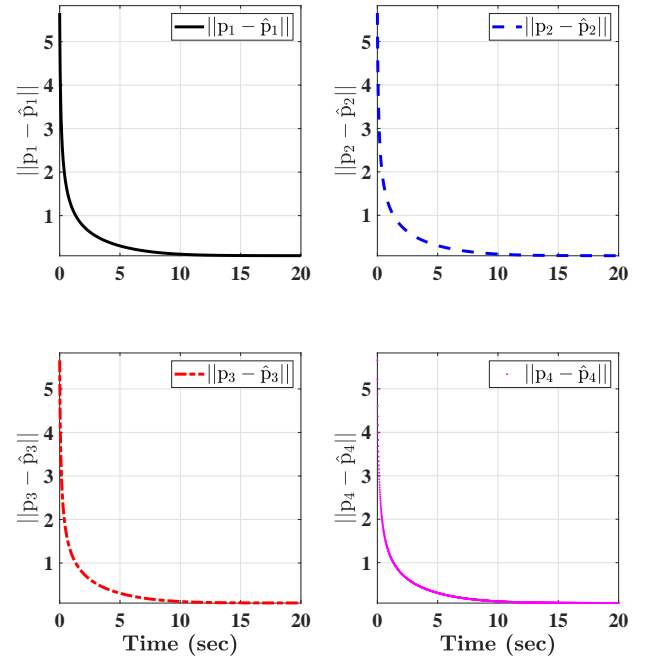


Fig. 4. Error trajectories of $\|p_i - \hat{p}_i\|$.

REFERENCES

- [1] H. A. Hashim, "Guaranteed performance nonlinear observer for simultaneous localization and mapping," *IEEE Control Systems Letters*, vol. 5, no. 1, pp. 91–96, 2021.
- [2] H. Choset, S. Walker, K. Eiamsa-Ard, and J. Burdick, "Sensor-based exploration: Incremental construction of the hierarchical generalized voronoi graph," *The International Journal of Robotics Research*, vol. 19, no. 2, pp. 126–148, 2000.

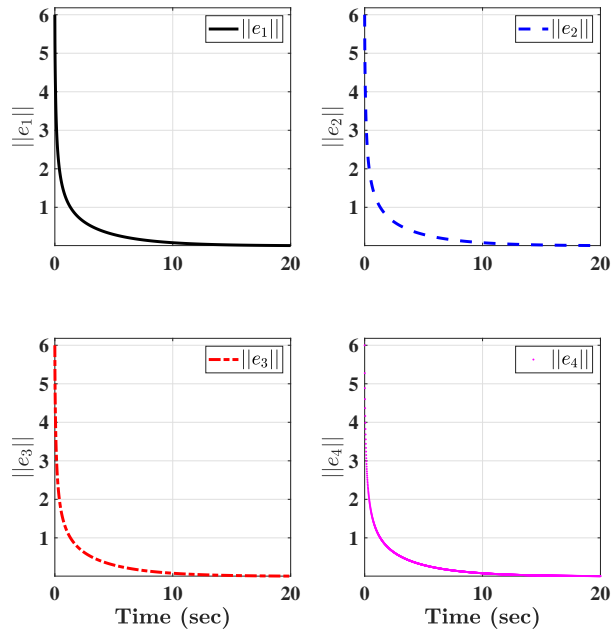


Fig. 5. Evolution of error trajectories of e_i .

- [3] H. Durrant-Whyte and T. Bailey, "Simultaneous localization and mapping: part i," *IEEE robotics & automation magazine*, vol. 13, no. 2, pp. 99–110, 2006.
- [4] K. E. Bekris, M. Glick, and L. E. Kavraki, "Evaluation of algorithms for bearing-only slam," in *Proceedings 2006 IEEE International Conference on Robotics and Automation, 2006. ICRA 2006*. IEEE, 2006, pp. 1937–1943.
- [5] A. J. Davison, I. D. Reid, N. D. Molton, and O. Stasse, "Monoslam: Real-time single camera slam," *IEEE transactions on pattern analysis and machine intelligence*, vol. 29, no. 6, pp. 1052–1067, 2007.
- [6] D. E. Zlotnik and J. R. Forbes, "Gradient-based observer for simultaneous localization and mapping," *IEEE Transactions on Automatic Control*, vol. 63, no. 12, pp. 4338–4344, 2018.
- [7] H. A. Hashim and A. E. E. Eltokhy, "Nonlinear filter for simultaneous localization and mapping on a matrix lie group using imu and feature measurements," *IEEE Transactions on Systems, Man, and Cybernetics: Systems*, vol. PP, no. PP, pp. 1–11, 2020.
- [8] M. Montemerlo and S. Thrun, *FastSLAM: A scalable method for the simultaneous localization and mapping problem in robotics*. Springer, 2007, vol. 27.
- [9] S. Huang and G. Dissanayake, "Convergence and consistency analysis for extended kalman filter based slam," *IEEE Transactions on robotics*, vol. 23, no. 5, pp. 1036–1049, 2007.
- [10] G. Dissanayake, S. Huang, Z. Wang, and R. Ranasinghe, "A review of recent developments in simultaneous localization and mapping," in *2011 6th International Conference on Industrial and Information Systems*. IEEE, 2011, pp. 477–482.
- [11] C. Cadena, L. Carlone, H. Carrillo, Y. Latif, D. Scaramuzza, J. Neira, I. Reid, and J. J. Leonard, "Past, present, and future of simultaneous localization and mapping: Toward the robust-perception age," *IEEE Transactions on robotics*, vol. 32, no. 6, pp. 1309–1332, 2016.
- [12] H. A. Hashim, L. J. Brown, and K. McIsaac, "Nonlinear stochastic attitude filters on the special orthogonal group 3: Ito and stratonovich," *IEEE Transactions on Systems, Man, and Cybernetics: Systems*, vol. 49, no. 9, pp. 1853–1865, 2019.
- [13] H. A. Hashim, "Systematic convergence of nonlinear stochastic estimators on the special orthogonal group SO(3)," *International Journal of Robust and Nonlinear Control*, vol. 30, no. 10, pp. 3848–3870, 2020.
- [14] H. A. Hashim, L. J. Brown, and K. McIsaac, "Nonlinear pose filters on the special euclidean group SE(3) with guaranteed transient and steady-state performance," *IEEE Transactions on Systems, Man, and Cybernetics: Systems*, pp. 1–14, 2019.
- [15] H. A. Hashim and F. L. Lewis, "Nonlinear stochastic estimators on the special euclidean group SE(3) using uncertain imu and vision measurements," *IEEE Transactions on Systems, Man, and Cybernetics: Systems*, vol. PP, no. PP, pp. 1–14, 2020.
- [16] H. A. H. Mohamed, "Nonlinear attitude and pose filters with superior convergence properties," *Ph. D, Western University*, 2019.
- [17] T. Lee, "Exponential stability of an attitude tracking control system on so (3) for large-angle rotational maneuvers," *Systems & Control Letters*, vol. 61, no. 1, pp. 231–237, 2012.
- [18] H. F. Grip, T. I. Fossen, T. A. Johansen, and A. Saberi, "Attitude estimation using biased gyro and vector measurements with time-varying reference vectors," *IEEE Transactions on Automatic Control*, vol. 57, no. 5, pp. 1332–1338, 2012.
- [19] H. A. Hashim, L. J. Brown, and K. McIsaac, "Nonlinear stochastic position and attitude filter on the special euclidean group 3," *Journal of the Franklin Institute*, vol. 356, no. 7, pp. 4144–4173, 2019.
- [20] D. E. Zlotnik and J. R. Forbes, "Higher order nonlinear complementary filtering on lie groups," *IEEE Transactions on Automatic Control*, vol. 64, no. 5, pp. 1772–1783, 2018.
- [21] H. Strasdat, "Local accuracy and global consistency for efficient visual slam," Ph.D. dissertation, Department of Computing, Imperial College London, 2012.
- [22] T. A. Johansen and E. Brekke, "Globally exponentially stable kalman filtering for slam with ahrs," in *2016 19th International Conference on Information Fusion (FUSION)*. IEEE, 2016, pp. 909–916.
- [23] M. D. Shuster, "A survey of attitude representations," *Navigation*, vol. 8, no. 9, pp. 439–517, 1993.
- [24] H. A. Hashim, "Special orthogonal group SO(3), euler angles, angle-axis, rodriguez vector and unit-quaternion: Overview, mapping and challenges," *arXiv preprint arXiv:1909.06669*, 2019.